In Vitro Mimicking of Estrous Cycle Stages in Porcine Oviduct Epithelium Cells: Estradiol and Progesterone Regulate Differentiation, Gene Expression, and Cellular Function 1

Authors: Chen, Shuai, Einspanier, Ralf, and Schoen, Jennifer

Source: Biology of Reproduction, 89(3)

Published By: Society for the Study of Reproduction

URL: https://doi.org/10.1095/biolreprod.113.108829

BIOLOGY OF REPRODUCTION (2013) **89**(3):54, 1–12
Published online before print 31 July 2013.
DOI 10.1095/biolreprod.113.108829

In Vitro Mimicking of Estrous Cycle Stages in Porcine Oviduct Epithelium Cells: Estradiol and Progesterone Regulate Differentiation, Gene Expression, and Cellular Function[1]

Shuai Chen, Ralf Einspanier, and Jennifer Schoen[2]

Institute of Veterinary Biochemistry, Department of Veterinary Medicine, Freie Universitaet Berlin, Berlin, Germany

ABSTRACT

Throughout the estrous cycle the oviduct epithelium undergoes dramatic morphological and functional changes. To elucidate cyclic cellular events and associated regulation mechanisms of 17beta estradiol (E2) and progesterone (P4), we mimicked estrous cycle stages in vitro using a culture system of primary porcine oviduct epithelium cells (POEC). Cells were polarized in an air/liquid interface and then treated with E2 and P4 for physiological time periods: In experiment 1, high concentration of P4 with low concentration of E2 for 10 days resembled diestrus; in experiment 2, following the previous diestrus, sequential high E2 with low P4 for 2.5 days represented estrus. Histomorphometry and electron microscopy showed cyclic changes in cellular height, cell population, and cilia density under the influence of hormone stimulation. Transepithelial electrical resistance was high in simulated diestrus but reduced in estrus. Thus, E2 and P4 affect cellular polarity, transformation of ciliated and secretory cells, as well as electrical conductivity of oviduct epithelium. Simulation of diestrus led to significant decrease in expression of hormone receptors *(PGR and ESR1*) and other epithelial markers (*MUC16, OVGP1,* and *HSP90B1*), while sequential simulated estrus caused an increase in these markers. The hormonal regulation of some marker genes was clearly time-dependent. Furthermore, POEC showed increased sperm-binding capacity in simulated estrus. In this study, we also present a novel approach based on the AndroVision software, which can be routinely utilized as a parameter for ciliary activity, and for the first time, we showed fluid movement patterns along the epithelium lining in vitro.

estrous cycle stages, fluid movement pattern, hormonal stimulation, oviduct epithelium, sperm binding

INTRODUCTION

The oviduct epithelium is mainly made up of ciliated and secretory cells, providing the micromilieu for fertilization and embryonic development as well as regulating gamete transport [1, 2]. Previous in vivo studies on sows, bitches, cows, and mares have revealed that oviduct epithelium undergoes dramatic morphological and functional changes throughout the estrous cycle [3–6]. In luteal phase, the oviduct epithelium exhibits a regressed status, characterized by substantial reduction in cellular height and marked deciliation. Conversely, cells reenter proliferative status in follicular phase, including a rise in epithelium height, a high portion of ciliated cells, and increased secretory activity. In the oviducts of primate species, similar changes have been demonstrated during the menstrual cycle [7]. Hormonal steroids, mainly 17β-estradiol (E2) and progesterone (P4), play pivotal roles in ciliogenesis and cell growth. However, the cyclic events within oviduct epithelium and associated regulation mechanisms of E2 and P4 at the cellular and molecular levels are still not clearly elucidated.

The caudal epithelium serves as a gamete reservoir and plays a significant role in sperm-epithelium interactions. It appears to lengthen the survival of sperm [8], regulate capacitation [9, 10], and synchronize sperm transit with ovulation [11]. In the past decades, conflicting reports have been published concerning the cycle-specific regulation of sperm binding. Several studies indicated estrous stages had no impact on sperm-binding patterns in bovine and porcine [12–14]. In contradiction to these findings, dependency of sperm binding on cyclic stage has been revealed in horses and rats [15, 16]. However, these studies were conducted on different models using cell vesicles, tissue explants, or animal models, which tend to create inconsistent findings.

Ciliary beating is an iconic feature regulating oviduct flow directions. Although the frequency of cilia beating has been assessed by high-speed camera-assisted video microscopy [17, 18], there is no available approach that provides information on fluid movement patterns over the luminal epithelium. Applying a technique that can be routinely used to track the liquid flow on the epithelium might bring more insight into mechanisms of cilia function.

So far, in vitro cultures of oviduct epithelial cells have been developed from several species (e.g., cows, sows, human, and monkeys) [19–23]. However, to our knowledge, there is no study on simulating estrous cycle events in these cultures, due either to the in vitro deprivation of morphological and functional characteristics [20, 23] or due to the limited culture duration [21].

Previously we established a culture method for the long-term cultivation of polarized porcine oviduct epithelium cells (POEC) [19]. In the present study, we aimed to mimic representative estrous cycle stages by periodical stimulation of the long-term cultures with E2 and P4, thus investigating the direct impact of E2 and P4 on the oviduct epithelium. In our simulation system, the morphological and ultrastructural characteristics were examined by histology and electron microscopy. Functional changes caused by the hormonal

[1]Supported by Federal Institute for Risk Assessment (BfR, FK 1329-473), Germany. S.C. was supported by the China Scholarship Council (CSC). Part of the work was presented in part at the 2nd Joint German-Polish Conference on Reproductive Medicine, 27 February–1 March, 2013, Gdansk, Poland.
[2]Correspondence: Schoen Jennifer, Institute of Veterinary Biochemistry, Department of Veterinary Medicine, Freie Universitaet Berlin, Oertzenweg 19b, 14163 Berlin, Germany.
E-mail: jennifer.schoen@fu-berlin.de

Received: 22 February 2013.
First decision: 26 March 2013.
Accepted: 1 July 2013.

eISSN: 1529-7268 http://www.biolreprod.org
ISSN: 0006-3363

treatment were investigated by gene expression analysis and examination of the sperm-epithelium binding capacity. Furthermore, we describe a novel method to monitor fluid movement patterns along the epithelium lining as a parameter for cilia activity.

MATERIALS AND METHODS

Chemicals and Reagents

Reduced glutathione, ascorbic acid, E2 (E8875) and P4 (P6149) were purchased from Sigma. All the media, as well as FBS (fetal bovine serum) superior (S0615, lot No.1119X), and cell culture additives (including penicillin/streptomycin, gentamycin, and amphotericin B) were supplied by Biochrom. Phenol red free Ham F12 medium was custom synthesized by the company. PeakFlow™ Carmine flow cytometry reference beads (P14831) and MitoTracker Red (M-7512) were purchased from Life Technology. AndrostarPLUS was obtained from Minitube. All the other reagents were obtained from Carl Roth unless otherwise indicated.

Culture of POEC

Porcine reproductive tracts were collected from 6-mo-old gilts (hybrids, German Large White × German Landrace) in the local abattoir (Vion Lausitz GmbH, Berlin, Germany) within 15 min after slaughter. Only the oviducts of noncycling gilts were selected. Isolation of primary oviduct epithelial cells was performed following the protocol previously described by our group [19]. Subsequently, cells were seeded at 3×10^5 cells/cm^2 onto Polyethylene Terephthalate (PET) Millicell inserts (Millipore), which were placed in culture plates with the culture medium placed at the basolateral side.

Because this study focused on effects of E2 and P4, phenol red free Ham F12 and FBS superior, which has low and defined hormone levels, were applied [24]. The certificate analysis provided by the manufacturer indicated FBS superior used in this study contained 21.3 pg/ml E2 and <0.2 ng/ml P4. The composition of the culture medium was as follows: phenol red free Ham F12 (containing 10% FBS) was enriched at 2:1 (v:v) with 3T3 conditioned media and then supplemented with 1% penicillin/streptomycin, 1 μg/ml amphotericin B, 50 μg/ml gentamycin, 10 μg/ml reduced glutathione, and 10 μg/ml ascorbic acid. The description for preparation of 3T3 conditioned media was given previously [19]. Cells were maintained in a chamber at 38°C with 5% CO_2. To achieve an air/liquid interface, medium inside the inserts was suctioned off 48 h after seeding. Afterward, medium in the basolateral compartment was changed twice every week.

Steroid Stimulation

Cultures were stimulated periodically with exogenous P4 and E2 from the basolateral side. The doses of E2 and P4 were selected based on physiological plasma hormone levels reported from sows in vivo [25, 26]. The estrous cycle simulation comprised two different experiments. We present the schematic time courses of these experiments in Figure 1.

Experiment 1: determination of preculture duration and simulation of diestrus. To determine the optimal stimulation strategy, POEC from eight animals were precultured for 11 or 32 days to allow building up of cellular polarity. Thereafter, cells were treated with 35 ng/ml P4 and 10 pg/ml E2 (final concentration) for 10 days to mimic diestrus. For the control group, cells were first subjected to the same preculture for 11 or 32 days and then treated with only steroid solvent (ethanol) for 10 days. The total culture duration therefore was either 3 or 6 wk. For each animal, POEC were seeded onto four inserts to allow both histological and mRNA analysis of diestrus and the control.

Experiment 2: simulation of diestrus and estrus. Because the results of experiment 1 indicated that POEC responded similarly to steroid stimulation after 11 and 32 days of preculture, the 11 day preculture duration was selected for experiment 2. POEC from six animals were used to simulate diestrus and estrus. As in experiment 1, cells were first precultured for 11 days and then underwent diestrus simulation for 10 days. To simulate estrus, subsequently cells were treated with 50 pg/ml E2 and 0.5 ng/ml P4 (final concentration) for 2.5 days. In the control group, cells were precultured for 11 days and then treated with steroid solvent only. In this experiment for histological evaluation of diestrus, estrus, and control, POEC were seeded onto three inserts per animal.

Previous reports have indicated that hormone responsiveness of bovine oviduct epithelial cells drops after 18 h of hormonal stimulation [21]. Therefore, to detect mRNA expression profiles, cells were seeded on four additional inserts per animal and underwent stimulation as described above. Cells were harvested after 10 days of diestrus simulation and after both 10 h and 2.5 days of estrus simulation. Control cells were harvested after 12.5 days of incubation with steroid solvent only.

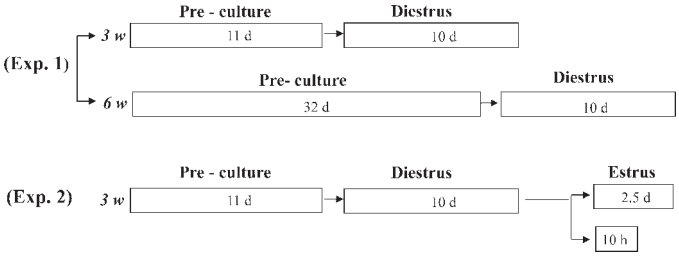

FIG. 1. Time course scheme of the simulation system for experiment 1 and experiment 2. During preculture, cells were grown in culture medium. Diestrus was simulated by medium supplementation with 35 ng/ml P4 and 10 pg/ml E2; to simulate estrus, medium was supplemented with 50 pg/ml E2 and 0.5 ng/ml P4. w, weeks; d, days; h, hours.

Transepithelial Electrical Resistance Assessment

To quantitatively assess the confluence and barrier formation of cultures, transepithelial electrical resistance (TEER) measurement was applied. The ohmic resistance was determined shortly before harvest of cultures using the EVOM^2 Epithelial Voltohmmeter (WPI). The unit area resistance value was calculated according to the manufacturer's description.

Histological Analysis and Electron Microscopy

After cultivation, membranes with cells were washed in PBS and fixed in Bouin solution. After removal from the inserts, membranes were first embedded in 2% agarose followed by postfixation in 4% formalin. After dehydration in an ascending ethanol series, the samples were embedded in paraplast. Three-micron sections were cut for haematoxylin/eosin (HE) staining, and only sections in the middle part of the membrane were collected for morphometric analysis. The height of the epithelial layer was measured by randomly taking three pictures from both ends and the middle part of the section. On each picture, the measurement was performed on five equidistant spots evenly distributed throughout the entire image. Thus, a total of 15 measurements were performed for each sample.

To monitor variation of cell population during simulation, five pictures were randomly taken for each sample. On each picture, we determined the total cell number per picture (membrane length per picture: 214 μm), as well as the number of secretory cells, which were characterized by extended protrusions. For electron microscopy, membranes were rinsed in PBS and fixed in 3% glutaraldehyde at 4°C overnight. Samples from three animals were processed in the Leibniz Institute for Zoo and Wildlife Research following standard procedures as described previously [19].

Expression of mRNA

Total RNA was extracted from POEC cultures using the mirVana miRNA Isolation Kit (Applied Biosystem). One microgram RNA was reverse transcribed by RevertAid reverse transcriptase (Fermentas) after DNase treatment. Quantitative PCR (qPCR) amplification was performed on the StepOne Plus cycler (Applied Biosystems) employing SensimixSYBR high-ROX kit (Bioline GmbH). The cycling program was: 1 cycle, 10 min at 95°C; 40 cycles, 95°C for 15 sec, corresponding annealing temperature for 20 sec, and 72°C for 30 sec. The efficiency and linearity of qPCR amplification were determined by standard curves (series dilution of purified PCR product). The geNorm software was used to normalize gene expression by computing the normalization factor based upon the geometric mean of four reference genes: actin, beta (*ACTB*); succinate dehydrogenase complex, subunit A, flavoprotein (Fp) (*SDHA*); tyrosine 3-monooxygenase/tryptophan 5-monooxygenase activation protein, zeta polypeptide (*YWHAZ*); and 18S ribosomal RNA (*18S rRNA*). All the primer sequences and corresponding annealing temperatures are listed in Table 1.

Preparation of Sperm

All the sperm samples were provided and preprocessed by the Unit for Reproductive Medicine of Clinics, University of Veterinary Medicine Hannover (Hannover, Germany). Briefly, semen samples were collected from one

TABLE 1. List of porcine primers used for qPCR analysis.

Gene symbol	Primer sequence (5′ to 3′)	Fragment size (bp)	Tm (°C)
ACTB	Forward: CAACTGGGACGACATGGAG	234	60
	Reverse: GAGTCCATCACGATGCCAG		
C3	Forward: AACAAGGGCAAGCTGTTGAAGGTG	119	60
	Reverse: TAATAAGCCACCAGGCGGAAGGAA		
ESR1	Forward: AGGGAAGCTCCTGTTTGCTCC	234	60
	Reverse: CGGTGGATATGGTCCTTCTCT		
GPER	Forward: GTGCCCGACCTGTACTTCAT	182	58
	Reverse: AAGCTCATCCAGGTGAGGAA		
HSP90B1	Forward: TCATGAAAGCCCAAGCCTACCAGA	195	60
	Reverse: CTGACCGCAGTGTTGCTGTTTCAA		
MKI67	Forward: CTCTTGTCCCTGAATCCGCA	138	60
	Reverse: TAGCGATGGAGGTAAGTGGC		
MUC 1	Forward: AGCTGATTCTGGCCTTCCAAGACA	96	60
	Reverse: TGGTCAGGTTATAGGTGCCTGCTT		
MUC 16	Forward: AGTGGCTATGCACCCCAGAC	191	60
	Reverse: ACCAGGCAGGAGCGGAATAC		
OVGP 1	Forward: TACTTGAAGAGCTCCTGCTTGCCT	134	60
	Reverse: TCTTCCCAGAAGGCGCACATCATA		
PGR	Forward: TGAGAGCACTAGATGCCGTTGCT	198	60
	Reverse: AGAACTCGAAGTGTCGGGTTTGGT		
SDHA	Forward: CTACAAGGGGCAGGTTCTGA	141	60
	Reverse: AAGACAACGAGGTCCAGGAG		
YWHAZ	Forward: TGATGATAAGAAAGGGATTGTGG	203	60
	Reverse: GTTCAGCAATGGCTTCATCA		
18S rRNA	Forward: AATCGGTAGTAGCGACGG	276	59
	Reverse: AGAGGGACAAGTGGCGTTC		

healthy boar with proven fertility. Samples were labeled with MitoTracker Red and then preserved in the commercial extender AndrostarPLUS. Sperm were delivered overnight at 20°C to the laboratory and applied to each experiment immediately after arrival.

To eliminate diluents, 10 ml of sperm were gently added on top of 5 ml of sucrose gradient in a falcon tube, and then centrifuged at 300 × *g* for 10 min followed by another 10 min at 750 × *g*. After aspirating the supernatant, the pellet was suspended in Medium 199 and adjusted to the density of 2×10^7 sperm/ml. After that, the sperm were incubated at 38°C for 10 min before placing inside the cell inserts, and motility and viability of sperm were assessed under the light microscope.

In Vitro Sperm-Binding Test

Cells were seeded onto transparent PET inserts (Millipore), and estrous cycle simulation was performed through 3 wk of culture (n = 3 animals) as described in experiment 2. Sperm were first diluted with Medium 199 (20×10^6 sperm/ml), and then 50 µl of the suspension was added on top of each membrane with cells. After 45 min of coincubation at 38°C, sperm suspension was removed; cells were washed twice with Medium 199 to remove floating sperm. Thereafter, sperm-bearing cultures were instantly inspected under the Axiovert 35 fluorescent microscope (Carl Zeiss). In each culture, seven fields (area 0.14 mm^2) along the diametral line of membrane were captured using AxioVison (Rel.4.8) software. Afterward, cocultures were fixed in 3% glutaraldehyde for scanning electron microscopy (SEM) observation. The amount of bound sperm was counted using ImageJ software. The binding index (BI) was defined as the number of sperm bound to 1 mm^2 of cell surface.

Tracking of Apical Fluid Movement

Estrous cycle was simulated as described in experiment 2 using POEC (n = 4 animals) seeded onto transparent inserts. Fluorescent beads with a diameter of 2.5 µm were diluted 1:20 in Ham F12 medium, and then 5 µl of suspension (6×10^3 beads) was added inside the insert. After the beads settled down, five fields of view were randomly chosen in each sample (n = 5 replicates) and a 10-sec video was taken in each field. The frame rate of the video was 50 frames/sec (avA1600-50gc; Basler). These videos were analyzed by the AndroVision software (Minitube), which automatically generated the traveling paths of the beads. In parallel, curvilinear velocity (VCL) and straight line velocity (VSL) of the beads were systematically calculated at the end of each video.

Statistical Analysis

Statistical evaluations in this study were performed using SPSS Statistics 20 for Windows. The normal distribution of data was tested by the Schapiro-Wilk method. In experiment 1, comparison of cellular height, TEER, cell counts, and qPCR data were all analyzed using the paired *t*-test. In experiment 2, we used one-way repeated measures ANOVA for analysis of cellular height, TEER, cell counts, qPCR data, sperm binding, and velocity of beads. The Greenhouse-Geisser correction was applied when $\varepsilon < 0.75$, and the Huyn-Feldt correction was applied when $\varepsilon > 0.75$. If repeated measures ANOVA indicated that the overall result was significant, Fisher least significant difference (LSD) post hoc tests were conducted. To further compare sperm binding across treatments of each animal, Kruskal-Wallis test (nonparametric ANOVA) was conducted followed by Mann-Whitney *U*-test. To further compare velocity of beads across treatments of each individual animal, one-way ANOVA was performed followed by Tukey post hoc analysis. In all the experiments, $P < 0.05$ was considered as significant.

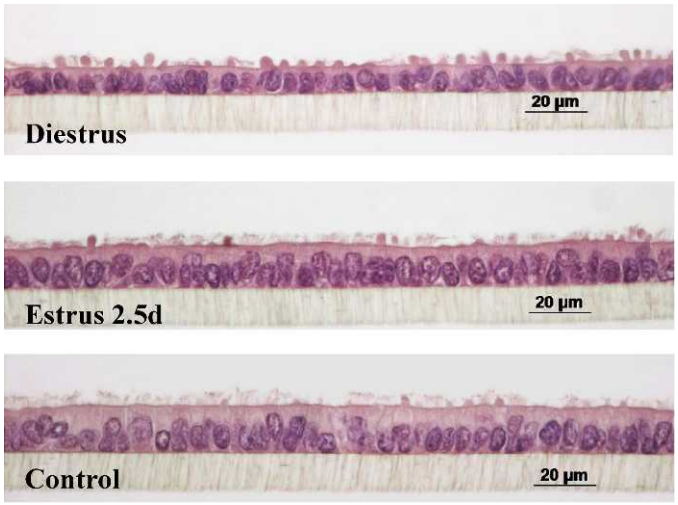

FIG. 2. Representative cross-sections of POEC cultures in different simulated cycle stages. HE staining, magnification ×400.

TABLE 2. Cellular height (μm) of POEC in different simulated cycle stages (mean ± SD) in experiment 1.*

	3 wk			6 wk		
Animal	Diestrus (D)	Control (C)	Ratio (D/C)	Diestrus (D)	Control (C)	Ratio (D/C)
A1	6.93 ± 1.72	14.13 ± 1.24	0.49	9.83 ± 0.66	17.05 ± 1.00	0.58
A2	8.85 ± 0.59	14.95 ± 0.73	0.59	11.88 ± 0.73	19.86 ± 1.08	0.60
A3	8.63 ± 1.40	14.70 ± 0.95	0.59	9.41 ± 0.78	14.48 ± 0.72	0.65
A4	9.49 ± 1.68	14.27 ± 0.63	0.67	10.37 ± 0.51	15.86 ± 1.07	0.65
A5	7.71 ± 0.44	12.67 ± 0.79	0.61	9.01 ± 0.73	16.82 ± 0.74	0.54
A6	9.01 ± 0.93	14.40 ± 0.72	0.63	12.69 ± 0.72	17.52 ± 1.60	0.72
A7	9.10 ± 1.13	14.59 ± 0.71	0.62	9.40 ± 0.83	16.95 ± 0.68	0.55
A8	8.66 ± 1.26	14.34 ± 0.72	0.60	9.71 ± 0.67	16.40 ± 1.02	0.59
Average	8.55 ± 0.78	14.25 ± 0.65	0.60	10.29 ± 1.31	16.87 ± 1.53	0.61
P value		$P < 0.001$			$P < 0.001$	

* Values represent means ± SD of 15 measurements, paired Student *t*-test.

RESULTS

Morphological Adaptions of Primary POECs in Response to Hormonal Stimuli

Histological evaluation clearly revealed morphological changes during estrous cycle simulation in POEC. In the control group, cells were polarized and maintained a mixed population of ciliated and secretory cells. In the simulated diestrus, P4-domination led to a dramatic decrease in cellular height. Cells were atrophied, appeared deciliated, and exhibited cuboidal shape. Besides, secretory cells with cytoplasmic protrusions extend the cellular boarder. Conversely, in the simulated estrus, cells regained columnar shape and showed dense cilia (Fig. 2).

In experiment 1, simulation of diestrus led to a highly significant decrease in cellular height in both 3 and 6 wk of culture (Table 2). The total cell numbers remained constant (Fig. 3). However, the proportion of secretory cells was significantly increased in simulated diestrus compared to the control in both 3 and 6 wk of culture. Morphological changes were accompanied by significant increase of cellular impedance in simulated diestrus as indicated by TEER measurement (Table 4).

In experiment 2, the same alternations in cellular height and TEER were detected in simulated diestrus (Tables 3 and 5). In the following estrous phase, subsequent treatment with high E2 and low P4 concentration caused a significant increase in cellular height. However, the cellular height in estrus was still relatively lower than in control cells (Table 3). TEER measurement showed that the cellular impedance in estrus was significantly lower than in diestrus (Table 5). There was no difference in total cell counts among the different groups ($F_{(2.0,\ 10.0)} = 0.18$, $P = 0.84$, Fig. 3C). Furthermore, qPCR analysis showed there was also no significant difference in mRNA-expression of the proliferation marker *MKI67* (antigen identified by monoclonal antibody Ki-67) among the different groups ($F_{(1.2,\ 6.2)} = 0.94$, $P = 0.39$, Fig. 3E). However, the composition of cell cultures was considerably altered by steroid stimulation. The portion of secretory cells was significantly different in all the groups ($F_{(2.0,\ 10.0)} = 130.64$, $P < 0.0001$). The highest numbers of secretory cells were found in diestrus, and the lowest in the control group (Fig. 3D).

SEM confirmed the ratio variation of ciliated and secretory cells from an aerial perspective (Fig. 4). The cilia were approximately 10 μm in length, reaching a level as found in vivo [27]. In the absence of exogenous E2 and P4, only few secretory cells extend beyond the apical boarder (Fig. 4C). In simulated diestrus, cytoplasmic protrusions of secretory cells were enlarged and dominated over the apical surface, which were interspersed with sparse straight cilia (Fig. 4D). In simulated estrus, cells became densely ciliated and exhibited swollen tips at the end of most cilia (Fig. 4E).

In spite of the predominance of secretory cells in diestrus, almost no secretory granules were found by transmission electron microscopy (TEM) in this stage (Fig. 4G). Estrus, however, was characterized by numerous electron-dense secretory granules and electron-light vacuoles in the supranuclear cytoplasm. They were well developed and large in size (Fig. 4H). A number of electron-dense granules were detected in the control cells as well (Fig. 4I). Kinocilia with typical 9+2 microtubules and mitochondria were observed in all the phases.

Functional Changes: Differential Gene Expression after Steroid Stimulation

Quantitative PCR analysis showed the dynamic changes in mRNA expression levels under steroid stimulation in both

TABLE 3. Cellular height (μm) of POEC in different simulated cycle stages (mean ± SD) in experiment 2.*

	3 wk			3 wk		
Animal	Diestrus (D)	Estrous 2.5 days (E)	Control (C)	Ratio (D/C)	Ratio (E/D)	Ratio (E/C)
A1	9.30 ± 1.11	13.31 ± 0.71	16.78 ± 1.12	0.55	1.43	0.79
A2	11.45 ± 0.97	14.82 ± 1.25	16.69 ± 1.25	0.69	1.29	0.89
A3	10.50 ± 1.42	13.67 ± 1.33	16.80 ± 1.72	0.63	1.30	0.81
A4	11.14 ± 1.22	15.27 ± 1.07	16.06 ± 1.49	0.69	1.37	0.95
A5	10.29 ± 1.04	13.72 ± 1.62	14.48 ± 0.95	0.71	1.33	0.95
A6	10.29 ± 0.70	13.00 ± 0.84	14.16 ± 0.93	0.73	1.26	0.92
Average	10.49 ± 0.75[a]	13.97 ± 0.89[b]	15.83 ± 1.20[c]	0.67	1.33	0.89
P value		$F_{(1.2,6.2)} = 75.3$, $P < 0.0001$				

* Values represent means ± SD of 15 measurements; repeated measures of ANOVA with LSD post hoc analysis.
[a,b,c] Between diestrus and control, $P < 0.001$; between diestrus and estrus, $P < 0.001$; between estrus and control, $P < 0.05$.

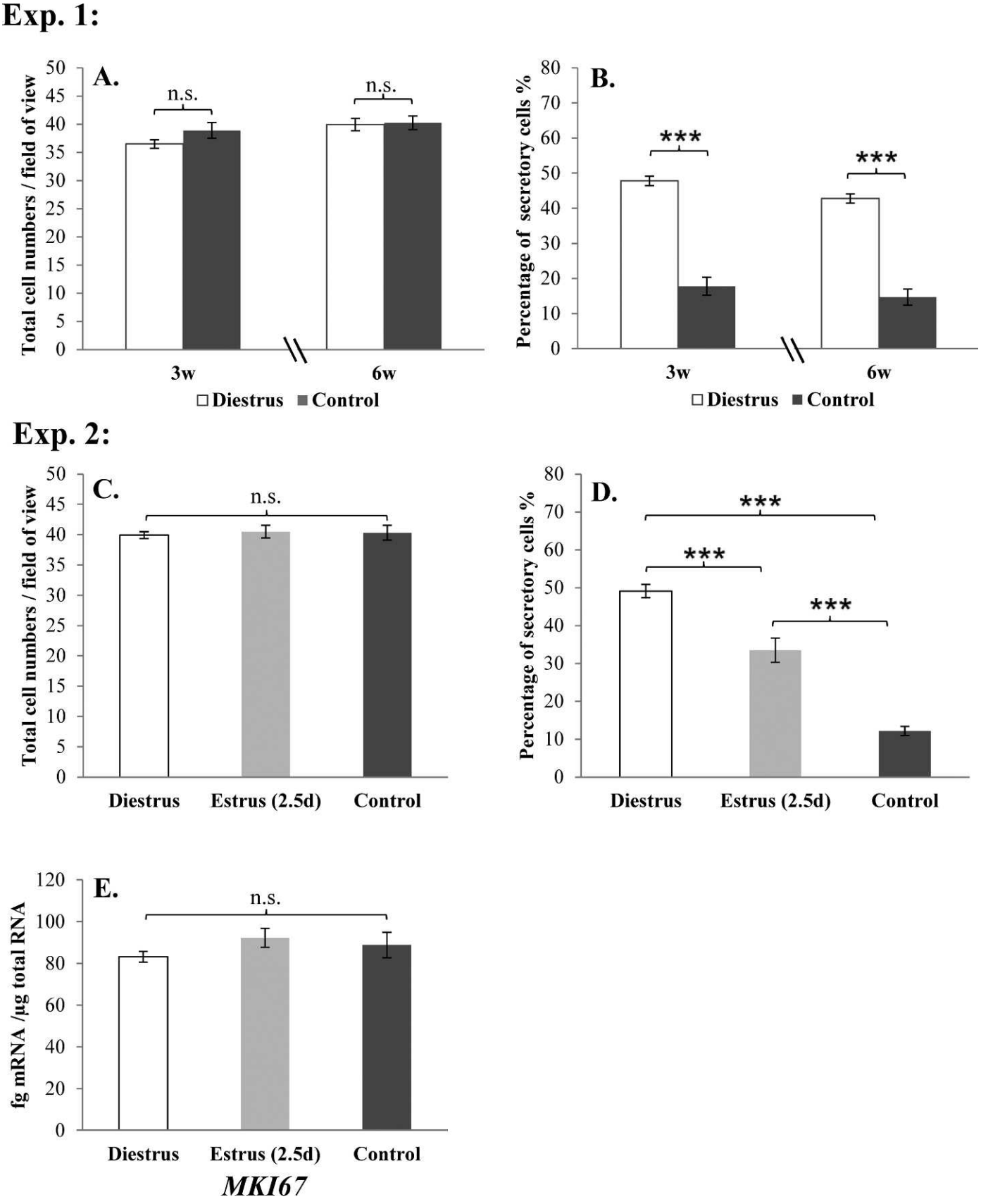

FIG. 3. Variation of cell populations during estrous cycle simulation. Experiment 1: total cell numbers/field of view remained constant (**A**) while percentage of secretory cells increased under P4 dominance (diestrus, **B**). Experiment 2: total cell number/field of view remained constant (**C**) while percentage of secretory cells increased after diestrus simulation and was gradually reduced after subsequent estrus simulation for 2.5 days (**D**); mRNA expression of MKI67 was not altered by hormonal treatment (**E**). Significance is indicated as ***$P < 0.001$, while n.s. represents no statistical difference.

TABLE 4. TEER ($\Omega \times cm^2$) of POEC in different simulated cycle stages in experiment 1.*

	3 wk			6 wk		
Animal	Diestrus (D)	Control (C)	Ratio (D/C)	Diestrus	Control	Ratio (D/C)
A1	1066.89	775.17	1.38	888.03	358.71	2.48
A2	988.68	754.38	1.31	876.15	647.79	1.35
A3	1126.62	731.94	1.54	918.72	840.18	1.09
A4	920.04	830.28	1.11	956.67	770.88	1.24
A5	911.79	865.92	1.05	987.36	771.21	1.28
A6	896.61	721.38	1.24	883.08	687.72	1.28
A7	951.39	703.89	1.35	880.77	693.99	1.27
A8	973.17	770.88	1.26	923.67	767.25	1.20
Average	979.40	769.23	1.27	914.31	692.22	1.40
P value		$P = 0.001$			$P = 0.002$	

* Paired Student *t*-test.

experiments. In experiment 1, simulation of diestrus (high P4 with low E2 for 10 days) led to significant decrease in expression of most selected genes. Expression levels of progesterone receptor (*PGR*), estrogen receptor 1 (*ESR1*), the oviduct secretory glycoproteins mucin 16 (*MUC16*), and oviductal glycoprotein 1 (*OVGP1*) as well as heat shock protein 90kDa beta (Grp94), member 1 (*HSP90B1*) were highly significantly downregulated under P4 dominance. The expression of these genes were 2-fold (*MUC16*) to 26-fold (*OVGP1*) higher in the control cultures compared to simulated diestrus (Table 6). Mucin 1 (*MUC1*) and G-protein-coupled estrogen receptor 1 (*GPER*) only showed moderate downregulation of less than 50% compared to the control. In contrast, expression of complement component 3 (*C3*) was significantly increased in simulated diestrus (Table 6).

In experiment 2, when comparing the simulated diestrus with control, we detected the same regulation patterns as in experiment 1. However, the downregulation of *GPER* and *MUC1* was not significant anymore (data not shown). In the subsequent 10 h estrus simulation, expression of *PGR, OVGP1, HSP90B1,* and *ESR1* were significantly increased. When estrus was extended for a physiological duration (2.5 days), a further increase in expression of *PGR* and *OVGP1* was detected compared to the 10 h stimulation. A significant upregulation of *MUC16* was detected only after 2.5 days estrus simulation. Expression of *MUC1, GPER,* and *C3* did not differ between simulated diestrus and estrus (Fig. 5).

Effects of Steroids on Sperm-Epithelium Interaction

Estrous stages were simulated in POEC from three gilts. After 45 min of coincubation, sperm were bound to the apical surface of POEC cultures. Motility of attached sperm was over 90% across all the groups. SEM demonstrated that sperm mainly adhered by the rostral region to the ciliated cells (Fig. 6, A and B). It can be discerned that sperm also attached to microvilli of secretory cells. However, this was only rarely seen in our cultures (Fig. 6C).

The sperm-binding capacity of the epithelium cultures differed in response to the hormonal treatment. In the simulated estrus, more sperm were bound compared to other groups. In two of three animals, the number of bound sperm in estrus was significantly higher than in diestrus (Table 7).

Fluid Movement Patterns Driven by Cilia Beating

Ciliary movement during the different cyclic stages was monitored in POEC cultures (n = 4 animals). Transport of fluorescent beads driven by cilia beating could be clearly visualized using the AndroVision software (for a representative video, see Supplementary Movie S1, available online at www.biolrerpod.org). The software automatically generated the typical trajectory of the beads. Figure 7 illustrates that beads were traveling along specific routes. Hence, the fluid movement had directional properties. The average bead transport speed varied between different animals: VCL ranged from 14.40 ± 3.10 μm/sec to 56.44 ± 10.18 μm/sec and VSL from 10.12 ± 3.02 μm/sec to 47.95 ± 3.43 μm/sec (Table 8). There was no significant difference in the VCL neither across treatment of each animal or across average values of all the animals. Although in two animals the VSL across treatments are significantly different, the trends were contradictory. In sum, no apparent difference was noted in VSL among simulated estrous stages.

TABLE 5. TEER ($\Omega \times cm^2$) of POEC in different simulated cycle stages in experiment 2.*

	3 wk			3 wk		
Animal	Diestrus (D)	Estrous 2.5 days (E)	Control (C)	Ratio (D/C)	Ratio (E/D)	Ratio (E/C)
A1	832.59	729.96	671.22	1.24	0.88	1.09
A2	883.74	829.62	723.69	1.22	0.94	1.15
A3	854.37	808.83	733.59	1.16	0.95	1.10
A4	1149.39	906.51	806.85	1.42	0.79	1.12
A5	1176.45	892.98	769.89	1.53	0.76	1.16
A6	1203.84	899.25	733.59	1.64	0.75	1.23
Average	1016.73[a]	844.53[b]	739.81[c]	1.37	0.84	1.14
P value		$F_{(1.0,\ 5.2)} = 18.85$, $P = 0.007$				

* Repeated measures ANOVA with LSD post hoc tests.
[a,b,c] Between diestrus and control, $P < 0.01$; between diestrus and estrus, $P < 0.05$; between estrus and control, $P < 0.01$.

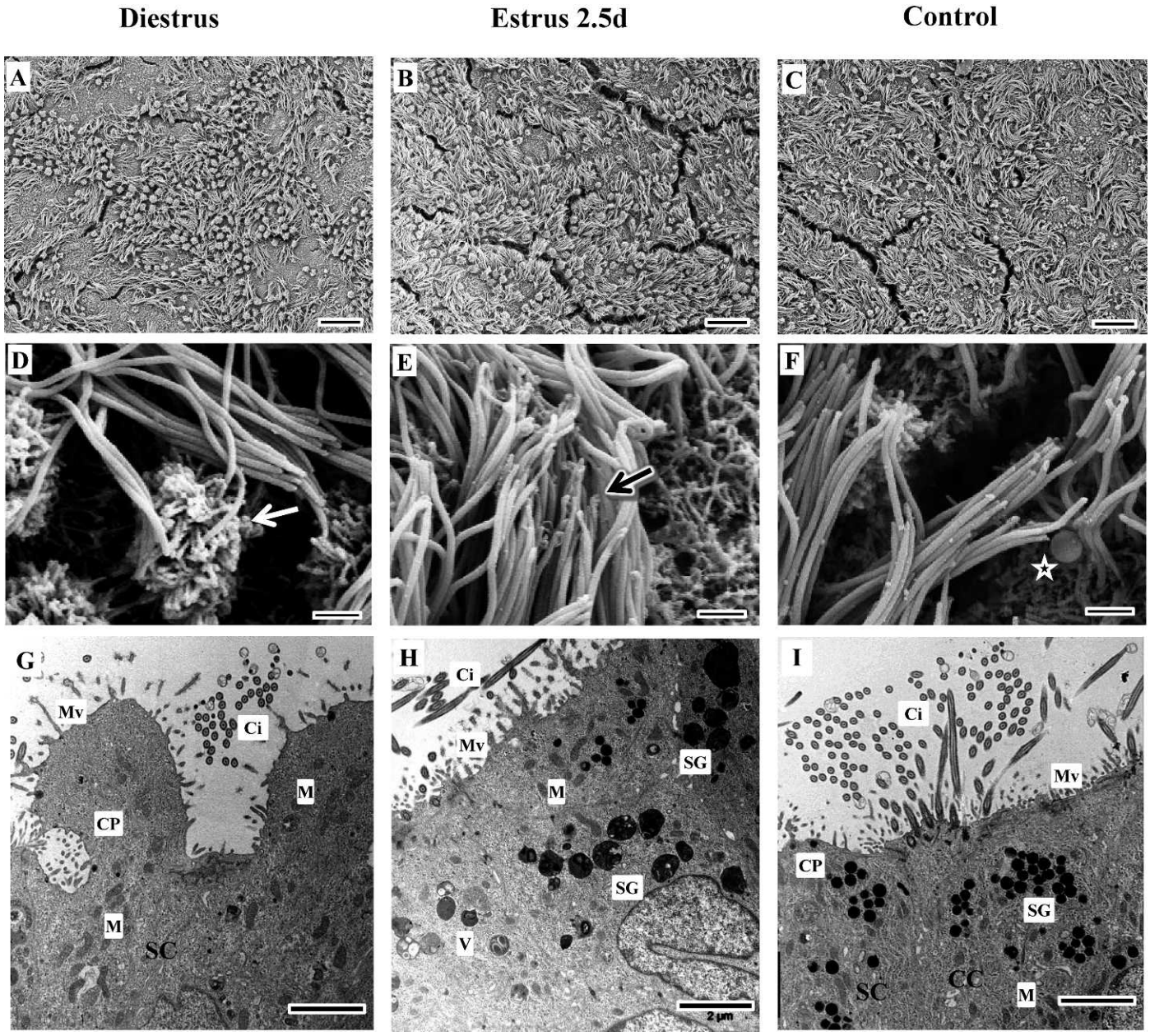

FIG. 4. Ultrastructural analysis of POEC during simulated estrous cycle in experiment 2. Scanning (**A**–**F**) and transmission (**G**–**I**) electron microscopic images of POEC. Arrowhead in **D** points to enlarged cytoplasmic protrusions of secretory cells. Arrowhead in **E** points to swollen tip of kinocilia. Star in **F** indicates secretory bubble. Bars in **A**–**C** = 20 µm and bars in **D**–**I** = 2 µm. CC, ciliated cells; SC, secretory cells; Ci, cilia; CP, cytoplasmic protrusions; M, mitochondria; Mv, microvilli; SG, electron-dense secretory granules; V, electron-light vesicles.

TABLE 6. Relative gene expression of POEC after diestrus simulation (experiment 1).*

	3 wk			6 wk		
Genes‡	Diestrus (D)	Control (C)†	*P* value	Diestrus (D)	Control (C)	*P* value
↓*PGR*	12.1 ± 2.96	100.00 ± 9.90	$P < 0.001$	32.32 ± 8.63	282.61 ± 68.55	$P < 0.001$
↓*ESR1*	35.46 ± 12.44	100.00 ± 10.19	$P < 0.001$	44.25 ± 9.36	125.47 ± 24.78	$P < 0.001$
↓*GPER*	62.91 ± 37.31	100.00 ± 14.77	$P < 0.05$	53.83 ± 10.40	84.90 ± 25.91	$P < 0.01$
↓*OVGP1*	4.22 ± 3.92	100.00 ± 19.92	$P < 0.001$	4.86 ± 3.49	130.36 ± 24.35	$P < 0.001$
↓*MUC1*	75.94 ± 22.64	100.00 ± 16.62	$P < 0.05$	59.60 ± 6.29	85.39 ± 20.81	$P < 0.01$
↓*MUC16*	48.18 ± 14.86	100.00 ± 15.7	$P < 0.001$	83.91± 12.58	159.45 ± 35.33	$P < 0.001$
↓*HSP90B1*	40.39 ± 17.02	100.00 ± 13.65	$P < 0.001$	37.82 ± 5.08	85.88 ± 15.73	$P < 0.001$
↑*C3*	154.93 ± 44.78	100.00 ± 33.33	$P < 0.05$	258.04 ± 34.58	148.15 ± 72.67	$P < 0.001$

* Expression levels are displayed relative to the 3-wk control group, and values represent mean ± SD, paired *t*-test.
† Expression level of the 3-wk control group was set at 100%.
‡ Downregulated gene indicated by ↓, and upregulated gene indicated by ↑.

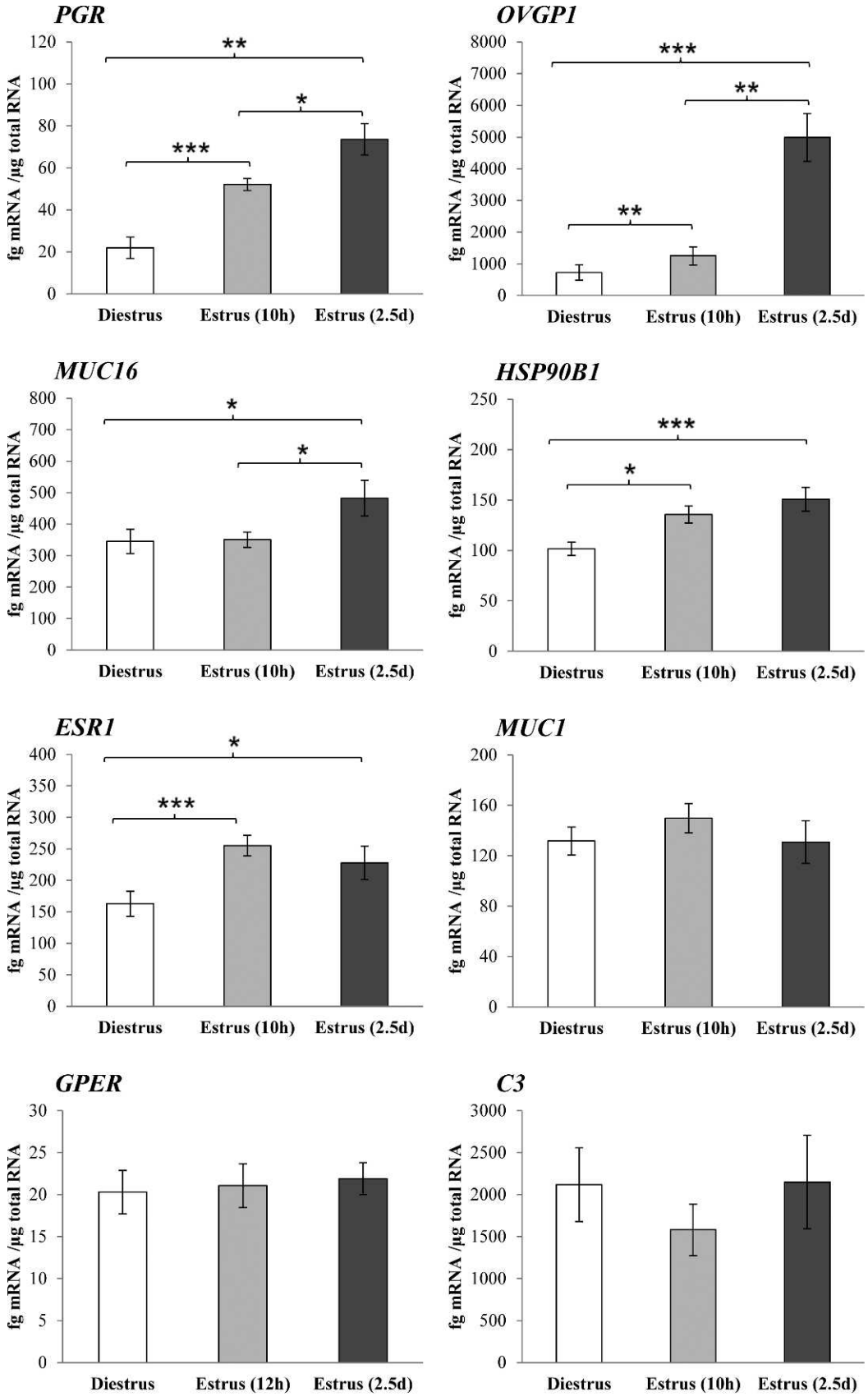

FIG. 5. Differential gene expression of marker genes after hormonal stimulation in experiment 2. Quantitative PCR analysis showed dynamic changes in mRNA expression levels under steroid stimulation. Data are analyzed by repeated measures of ANOVA followed by LSD post hoc tests. *PGR*: $F_{(1.2,\ 6.2)} = 26.80$, $P = 0.001$; *OVGP1*: $F_{(1.0,\ 5.1)} = 42.39$, $P = 0.001$; *MUC16*: $F_{(2.0,\ 10.0)} = 10.22$, $P = 0.004$; *HSP90B1*: $F_{(2.0,\ 10.0)} = 16.24$, $P < 0.001$; *ESR1*: $F_{(1.1,\ 5.5)} = 20.06$, $P = 0.005$; *MUC1*: $F_{(1.4,\ 7.2)} = 1.26$, $P = 0.32$; *GPER*: $F_{(2.0,\ 10.0)} = 0.50$, $P = 0.62$; *C3*: $F_{(1.3,\ 6.5)} = 3.75$, $P = 0.092$; Significance between two groups is indicated as $^{*}P < 0.05$, $^{**}P < 0.01$, and $^{***}P < 0.001$.

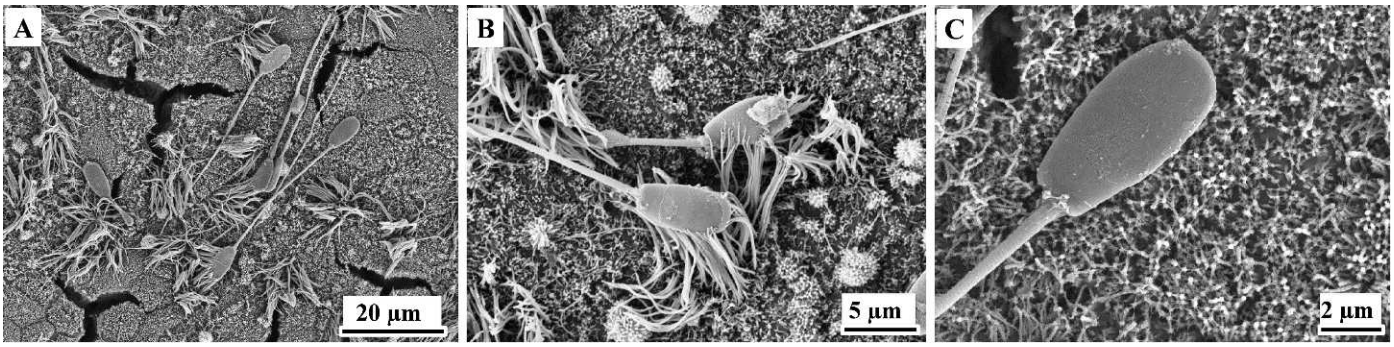

FIG. 6. Estrous cycle-dependent sperm-oviduct interaction in POEC during stimulation. **A**–**C**) SEM showing the contact between sperm and POEC. **A**) Sperm attached mainly by the rostral region. **B**) Strong binding between the cilia and the acrosomal region of sperm. **C**) Sperm attached to nonciliated cells. Bars = 20 μm (**A**), 5 μm (**B**), and 2 μm (**C**).

DISCUSSION

In this study, for the first time we mimicked estrous cycle stages on oviduct epithelium cells in vitro. This was achieved solely through administration of exogenous E2 and P4 in POEC cultures. Our simulation system has several advantages: first, the stimulation was feasible for physiological time duration; second, the system was highly reproducible; and third, it is a dynamic system, which constantly adjusted in cell population and cell morphology to steroid hormones.

Because cells were only treated by varying amount of E2 and P4, the cyclic changes revealed by histological and ultrastructural analysis provide direct evidence to the regulation effect of E2 and P4 on cellular polarization and cell composition in vitro. Total cell numbers remained constant regardless of the hormonal stimulation. Consistent with this finding, mRNA expression of *MKI67*, a marker for cell proliferation, also indicated the cell division status was unaltered during stimulation. However, the ratio of ciliated and secretory cells significantly changed in response to hormonal treatment. This suggests that the relative amount of E2 and P4 controlled the transformation between ciliated and secretory cells as well as induction of ciliogenesis in oviduct epithelium cells. Similar results were reported earlier for ovariectomized quail stimulated with different concentrations of P4 and E2 [28].

In our study, 59 out of 60 cultures developed TEER values ranging from 647 $\Omega \times cm^2$ to 1203 $\Omega \times cm^2$, which indicates the establishment of cellular polarity and barrier formation. A similar transepithelial resistance has been reported for monkey oviduct epithelium in vitro and in vivo [23]. Furthermore, we found the transcellular impedance was high in the simulated diestrus (P4-domination) and then decreased gradually in simulated estrus (E2-domination). Although in vivo impedance has rarely been investigated in oviduct, similar cyclic changes have been reported for the vagina and vulva [29, 30]. In our model, E2 and P4 showed effects on cellular electrical conductivity, which might be associated with the status of secretory activities and transcellular/paracellular transportation. TEM showed more secretory granules in estrus (E2-domination) and control (absence of E2 and P4), which might be associated with high expression of secretion-related genes (such as *OVGP1* and *MUC16)* in these two groups.

Previous studies showed that cycle stages and changing hormone levels affected gene expression in oviductal epithelium in vitro and ex vivo [21, 31, 32]. In experiment 1, we demonstrated that P4-domination downregulated the expression of most genes, including hormone receptors and secretory glycoproteins. This finding is in line with microarray results from the bovine oviduct [31]. Among all the selected genes, only *C3* showed an opposite response profile. Therefore, we hypothesize that *C3* is positively regulated by P4 in the oviduct. In experiment 2, the expression of most genes was higher in the simulated estrus compared to diestrus. At this point, it is not clear whether this upregulation is caused by the lower P4 concentration in the medium or reflects an E2 effect.

OVGP1 (MUC9) and *MUC16* are the major mucins secreted by oviduct epithelium cells [33], whereas *HSP90B1* regulates protein secretion and protein folding. The elevated expression of these genes might reflect activated secretion in simulated estrus. Increased expression of the hormone receptors *PGR* and *ESR1* in simulated estrus is again consistent with in vivo studies on bovine oviduct [31, 32].

GPER (a membrane estrogen receptor [34], which is rarely investigated in the oviduct) was slightly but significantly downregulated under P4-domination as detected in our first experiment. The study by Otto et al. [35] on *GPER* knockout mice indicated *GPER* is not essential for reproduction. In our model, *GPER* mRNA expression was regulated at least by P4, which points toward a role of *GPER* in the response of oviduct epithelium cells to hormonal stimuli. However, simulated estrus with lower levels of P4 and higher levels of E2 did not lead to significant changes in the expression levels of neither *GPER* nor *MUC1,* suggesting that even low levels of P4 (as

TABLE 7. Sperm BI during different simulated cycle stages.*

Animal	Diestrus	Estrus (2.5 days)	Control
A1	398.98 ± 42.58^{a}	754.08 ± 52.92^{b}	665.31 ± 41.72^{bc}
A2	687.76 ± 83.19	957.14± 130.15	803.06 ± 88.12
A3	376.53 ± 122.26^{a}	714.29 ± 140.85^{b}	401.02 ± 76.05^{ab}
Average	487.76 ± 100.21^{A}	808.50 ± 75.20^{B}	623.13 ± 117.96^{AB}
P value	$F_{(2.0,\ 4.0)} = 15.34$, $P = 0.013$		

* LSD post hoc test indicates significant difference between diestrus and estrus group ($^{A,B}P = 0.007$). For comparison across treatments of an individual animal, Kruskal–Wallis test was performed ($^{a,b,c}P < 0.05$). Values represent mean ± SEM.

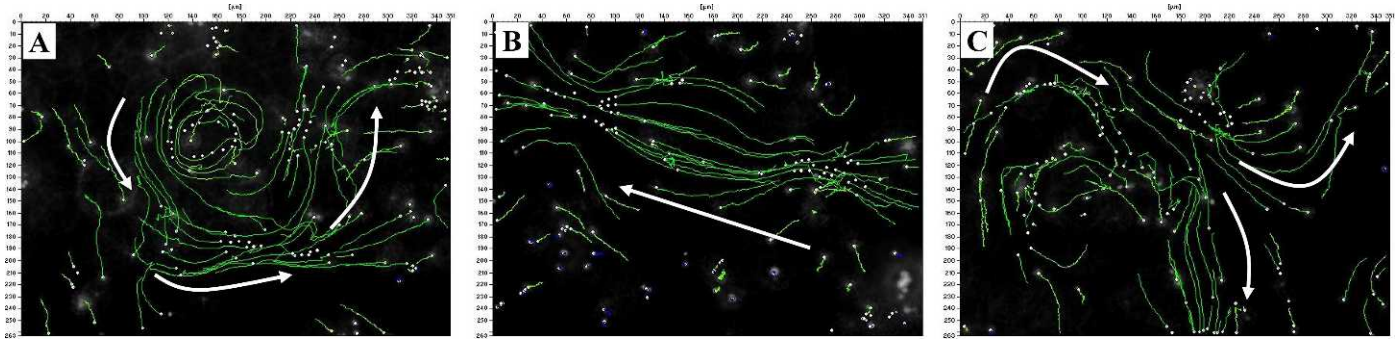

FIG. 7. Fluid movement patterns over the epithelium lining monitored by the AndroVision system tracking the transport path of fluorescent beads for 10 sec. Beads traveled along three typical paths: in circles (**A**), in straight lines (**B**), or in arcs (**C**). Direction of liquid movement was pointed out by arrows. Magnification ×200.

present in diestrus) downregulate expression of these genes and that E2 does not have a significant effect on the expression levels. When comparing 10 h of estrus simulation to 2.5 days of estrus simulation, the gene expression alterations showed different patterns: a time-dependent, long-term effect on *PGR, OVGP1,* and *MUC16* expression, but a rapid and short-term regulation of *ESR1* and *HSP90B1*.

In addition to presenting a phenocopy of the estrous cycle, we also aimed to investigate the functional changes in sperm-epithelium interaction. In our study, the binding was to both ciliated and secretory cells but preferentially to the ciliated type, which reflected previous research [15, 36]. Electron micrographs showed binding between cilia and the rostral aspect of the sperm, proving that cells in our system recapitulate the biological function of oviduct epithelium in vivo. Furthermore, our data support the notion that variation of hormone levels throughout the estrous cycle affects sperm-oviduct interaction. Previous studies in gilts demonstrated that exogenous E2 treatment increased sperm binding to oviduct explants [12]. Also in our study, more sperm bound to cells in simulated estrus. The low binding in P4-dominant group is in line with the report of Bureau et al. [37] who demonstrated that P4 pretreatment of porcine oviduct epithelial cells compromises sperm binding. In general, we propose the stage-specific binding might be a result of two mechanisms. The first is the varying numbers of ciliated cells during estrous cycle. Because most sperm were found trapped by cilia, the high degree of ciliation would probably promote the binding process in the estrous phase. The second is the observed changes in the composition and volume of oviduct secretion. It has been reported that activities of glycosidases in the oviduct fluid differ throughout the cycle [38]. The sperm-oviduct interaction is a carbohydrate-mediated process [39, 40]. Changes in glycosidase activities could act upon carbohydrate residues, thereby regulating the sperm binding.

For the first time, we adapted the AndroVision software for an epithelium cell culture model and developed a new analytic system that could be routinely used to investigate ciliary activity. In addition, we provide the first data on fluid movement patterns along the epithelium lining. Taking advantage of the cell model, the signal/noise ratio and image resolutions were substantially improved compared to other methods [18, 41]. The transport of beads proved that our culture is a dynamic system with vigorous ciliary activity. Besides, we demonstrated the directivity of the basal fluid stream guided by cilia beating. We consider that this information would facilitate studies on oviductal transport mechanisms of gametes and embryos [2]. Furthermore, this method allowed mathematical analysis of the speed of fluid movement. There were conflicting reports concerning ciliary activities throughout the cycle. One study showed changes in ciliary beating frequency (CBF) during the menstrual cycle in human [42]. Nishimura et al. [17, 18] reported that the CBF was controlled by steroid hormones during cycle in guinea pigs. However, the most recent studies revealed the specificity of ciliary beating can be attributed to anatomical positions rather than cyclic stages [41, 43]. In our study, the speed of beads transport was relatively constant in all the animals and corresponded to levels reported in murine oviduct and trachea [43]. No difference was noted in the speed of beads transport within different groups. This supports the deduction that tubal clearance of secretions takes priority over gamete transport. Nevertheless, experimental conditions such as pH values [44], vibration artifacts, and fluid volume might skew results. Therefore, further standardization of the analysis conditions is needed.

TABLE 8. Velocity parameters of beads in the apical fluid layer during different cyclic stages.*

	VCL†			VSL‡		
Animal	Diestrus	Estrus (2.5 days)	Control	Diestrus	Estrus (2.5 days)	Control
A1	26.87 ± 3.39	16.96 ± 3.68	14.40 ± 3.10	22.04 ± 2.58[a]	11.74 ± 3.33[ab]	10.12 ± 3.02[b]
A2	22.68 ± 3.97	24.45 ± 3.68	22.88 ± 5.06	20.36 ± 3.47	19.04 ± 3.25	19.56 ± 4.13
A3	19.39 ± 3.31	18.24 ± 1.86	31.36 ± 5.37	13.08 ± 3.34[a]	13.32 ± 1.98[a]	26.51 ± 4.60[b]
A4	52.80 ± 8.94	56.44 ± 10.18	52.60 ± 3.94	44.89 ± 8.11	46.52 ± 6.81	47.95 ± 3.43
Average	30.43 ± 3.92	29.02 ± 4.55	30.31 ± 3.85	24.71 ± 3.59	22.66 ± 3.76	25.62 ± 3.73
P value		$F_{(2.0,\ 6.0)} = 0.07$, $P = 0.93$			$F_{(2.0,\ 6.0)} = 0.29$, $P = 0.76$	

* Values represent means ± SEM. Repeated measures ANOVA to compare average values of all the groups. For comparison across treatments of an individual animal, one-way ANOVA with Tukey post hoc test was performed ($^{a,b}P < 0.05$).

† The speed (μm/sec) that beads traveled across the curved line from the beginning to the end of the analysis period.

‡ The speed (μm/sec) that beads traveled in a straight line from the beginning to the end of the analysis period.

In conclusion, for the first time we demonstrate the simulation of estrous cycle stages on mammalian oviduct epithelial cells in vitro and clearly showed the effect of E2 and P4 on differentiation, gene expression, and cellular function in oviduct epithelium. Because specific functions of oviduct epithelium are obtained under defined hormonal conditions, the in vitro simulation system will boost investigations on precisely timed local biological events occurring throughout the sexual cycle. Finally, the new approach for cilia movement analysis could be utilized to decipher basic transport mechanisms as well as human ciliary diseases, such as Kartagener syndrome, immotile cilia syndrome, ectopic pregnancy, and the influence of infections on cilia activity [2, 45].

ACKNOWLEDGMENT

We thank the Vion Lausitz GmbH, Kasel-Golzig, Germany, for providing tissue samples. We thank Dr. Gudrun Wibbelt and Dagmar Viertel, Leibniz Institute for Zoo and Wildlife research, Berlin, Germany, for their assistance in electron microscopy. We are very grateful to Prof. Dr. Dagmar Waberski, Dr. Heiko Henning, and Jenny Franz, Unit for Reproductive Medicine of Clinics, University of Veterinary Medicine Hannover, Germany, for providing porcine sperm and support in sperm preparation. We thank the Minitube Company, Tiefenbach, Germany, for providing the AndroVision software and associated equipment.

REFERENCES

1. Killian GJ. Evidence for the role of oviduct secretions in sperm function, fertilization and embryo development. Anim Reprod Sci 2004; 82–83: 141–153.
2. Lyons RA, Saridogan E, Djahanbakhch O. The reproductive significance of human fallopian tube cilia. Hum Reprod Update 2006; 12:363–372.
3. Abe H, Hoshi H. Regional and cyclic variations in the ultrastructural features of secretory cells in the oviductal epithelium of the Chinese Meishan pig. Reprod Domest Anim 2007; 42:292–298.
4. Steinhauer N, Boos A, Gunzel-Apel AR. Morphological changes and proliferative activity in the oviductal epithelium during hormonally defined stages of the oestrous cycle in the bitch. Reprod Domest Anim 2004; 39:110–119.
5. Aguilar JJ, Cuervo-Arango J, Mouguelar H, Losinno L. Histological characteristics of the equine oviductal mucosa at different reproductive stages. J Equine Vet Sci 2012; 32:99–105.
6. Abe H, Oikawa T. Observations by scanning electron microscopy of oviductal epithelial cells from cows at follicular and luteal phases. Anat Rec 1993; 235:399–410.
7. Donnez J, Casanas-Roux F, Caprasse J, Ferin J, Thomas K. Cyclic changes in ciliation, cell height, and mitotic activity in human tubal epithelium during reproductive life. Fertil Steril 1985; 43:554–559.
8. Kawakami E, Kashiwagi C, Hori T, Tsutsui T. Effects of canine oviduct epithelial cells on movement and capacitation of homologous spermatozoa in vitro. Anim Reprod Sci 2001; 68:121–131.
9. Tienthai P, Johannisson A, Rodriguez-Martinez H. Sperm capacitation in the porcine oviduct. Anim Reprod Sci 2004; 80:131–146.
10. Fazeli A, Elliott RM, Duncan AE, Moore A, Watson PF, Holt WV. In vitro maintenance of boar sperm viability by a soluble fraction obtained from oviductal apical plasma membrane preparations. Reproduction 2003; 125:509–517.
11. Topfer-Petersen E, Wagner A, Friedrich J, Petrunkina A, Ekhlasi-Hundrieser M, Waberski D, Drommer W. Function of the mammalian oviductal sperm reservoir. J Exp Zool 2002; 292:210–215.
12. Suarez S, Redfern K, Raynor P, Martin F, Phillips DM. Attachment of boar sperm to mucosal explants of oviduct in vitro: possible role in formation of a sperm reservoir. Biol Reprod 1991; 44:998–1004.
13. Lefebvre R, Chenoweth PJ, Drost M, LeClear CT, MacCubbin M, Dutton JT, Suarez SS. Characterization of the oviductal sperm reservoir in cattle. Biol Reprod 1995; 53:1066–1074.
14. Petrunkina AM, Gehlhaar R, Drommer W, Waberski D, Topfer-Petersen E. Selective sperm binding to pig oviductal epithelium in vitro. Reproduction 2001; 121:889–896.
15. Thomas PG, Ball BA, Brinsko SP. Interaction of equine spermatozoa with oviduct epithelial cell explants is affected by estrous cycle and anatomic origin of explant. Biol Reprod 1994; 51:222–228.
16. Orihuela PA, Ortiz ME, Croxatto HB. Sperm migration into and through the oviduct following artificial insemination at different stages of the estrous cycle in the rat. Biol Reprod 1999; 60:908–913.
17. Nakahari T, Nishimura A, Shimamoto C, Sakai A, Kuwabara H, Nakano T, Tanaka S, Kohda Y, Matsumura H, Mori H. The regulation of ciliary beat frequency by ovarian steroids in the guinea pig fallopian tube: interactions between oestradiol and progesterone. Biomed Res 2011; 32: 321–328.
18. Nishimura A, Sakuma K, Shimamoto C, Ito S, Nakano T, Daikoku E, Ohmichi M, Ushiroyama T, Ueki M, Kuwabara H, Mori H, Nakahari T. Ciliary beat frequency controlled by oestradiol and progesterone during ovarian cycle in guinea-pig fallopian tube. Exp Physiol 2010; 95:819–828.
19. Miessen K, Sharbati S, Einspanier R, Schoen J. Modelling the porcine oviduct epithelium: a polarized in vitro system suitable for long-term cultivation. Theriogenology 2011; 76:900–910.
20. Schoen J, Bondzio A, Topp K, Einspanier R. Establishment and characterization of an adherent pure epithelial cell line derived from the bovine oviduct. Theriogenology 2008; 69:536–545.
21. Rottmayer R, Ulbrich SE, Kolle S, Prelle K, Neumueller C, Sinowatz F, Meyer HH, Wolf E, Hiendleder S. A bovine oviduct epithelial cell suspension culture system suitable for studying embryo-maternal interactions: morphological and functional characterization. Reproduction 2006; 132:637–648.
22. Levanon K, Ng V, Piao HY, Zhang Y, Chang MC, Roh MH, Kindelberger DW, Hirsch MS, Crum CP, Marto JA, Drapkin R. Primary ex vivo cultures of human fallopian tube epithelium as a model for serous ovarian carcinogenesis. Oncogene 2010; 29:1103–1113.
23. Rajagopal M, Tollner TL, Finkbeiner WE, Cherr GN, Widdicombe JH. Differentiated structure and function of primary cultures of monkey oviductal epithelium. In Vitro Cell Dev Biol Anim 2006; 42:248–254.
24. Wesierska-Gadek J, Schreiner T, Maurer M, Waringer A, Ranftler C. Phenol red in the culture medium strongly affects the susceptibility of human MCF-7 cells to roscovitine. Cell Mol Biol Lett 2007; 12:280–293.
25. Henricks DM, Guthrie HD, Handlin DL. Plasma estrogen, progesterone and luteinizing hormone levels during the estrous cycle in pigs. Biol Reprod 1972; 6:210–218.
26. Peralta LE, Olarte MR, Arganaraz M, Ciocca D, Miceli DC. Progesterone receptors: their localization, binding activity and expression in the pig oviduct during follicular and luteal phases. Domest Anim Endocrinol 2005; 28:74–84.
27. Satir P. Mechanisms of ciliary movement: contributions from electron microscopy. Scanning Microsc 1992; 6:573–579.
28. Sandoz D, Biosvieux-Ulrich E, Laugier C, Brard E. Ciliogenesis in the mucous cells of the quail oviduct. II. Hormonal control [in French].J Cell Biol 1976; 71:460–471.
29. Rezac P, Kukla R, Poschl M. Effect of sow parity on vaginal electrical impedance. Anim Reprod Sci 2002; 72:223–234.
30. Rezac P, Olic I. Relationship between opposite changes of vaginal and vestibular impedance during estrous cycle in sows. Theriogenology 2006; 66:868–876.
31. Ulbrich SE, Kettler A, Einspanier R. Expression and localization of estrogen receptor alpha, estrogen receptor beta and progesterone receptor in the bovine oviduct in vivo and in vitro. J Steroid Biochem Mol Biol 2003; 84:279–289.
32. Bauersachs S, Rehfeld S, Ulbrich SE, Mallok S, Prelle K, Wenigerkind H, Einspanier R, Blum H, Wolf E. Monitoring gene expression changes in bovine oviduct epithelial cells during the oestrous cycle. J Mol Endocrinol 2004; 32:449–466.
33. Kadam KM, D'Souza SJ, Natraj U. Identification of cellular isoform of oviduct-specific glycoprotein: role in oviduct tissue remodeling? Cell Tissue Res 2007; 330:545–556.
34. Thomas P, Pang Y, Filardo EJ, Dong J. Identity of an estrogen membrane receptor coupled to a G protein in human breast cancer cells. Endocrinology 2005; 146:624–632.
35. Otto C, Fuchs I, Kauselmann G, Kern H, Zevnik B, Andreasen P, Schwarz G, Altmann H, Klewer M, Schoor M, Vonk R, Fritzemeier KH. GPR30 does not mediate estrogenic responses in reproductive organs in mice. Biol Reprod 2009; 80:34–41.
36. Vigil P, Salgado AM, Cortes ME. Ultrastructural interaction between spermatozoon and human oviductal cells in vitro. J Electron Microsc (Tokyo) 2012; 61:123–126.
37. Bureau M, Bailey JL, Sirard M-A. Binding regulation of porcine spermatozoa to oviductal vesicles in vitro. J Androl 2002; 23:188–193.
38. Carrasco LC, Romar R, Aviles M, Gadea J, Coy P. Determination of glycosidase activity in porcine oviductal fluid at the different phases of the estrous cycle. Reproduction 2008; 136:833–842.
39. Talbot P, Shur BD, Myles DG. Cell adhesion and fertilization: steps in

oocyte transport, sperm-zona pellucida interactions, and sperm-egg fusion. Biol Reprod 2003; 68:1–9.
40. Taylor U, Rath D, Zerbe H, Schuberth HJ. Interaction of intact porcine spermatozoa with epithelial cells and neutrophilic granulocytes during uterine passage. Reprod Domest Anim 2008; 43:166–175.
41. Kolle S, Dubielzig S, Reese S, Wehrend A, Konig P, Kummer W. Ciliary transport, gamete interaction, and effects of the early embryo in the oviduct: ex vivo analyses using a new digital videomicroscopic system in the cow. Biol Reprod 2009; 81:267–274.
42. Lyons RA, Djahanbakhch O, Mahmood T, Saridogan E, Sattar S, Sheaff MT, Naftalin AA, Chenoy R. Fallopian tube ciliary beat frequency in relation to the stage of menstrual cycle and anatomical site. Hum Reprod 2002; 17:584–588.
43. Noreikat K, Wolff M, Kummer W, Kolle S. Ciliary activity in the oviduct of cycling, pregnant, and muscarinic receptor knockout mice. Biol Reprod 2012; 86:120.
44. Salathe M. Regulation of mammalian ciliary beating. Annu Rev Physiol 2007; 69:401–422.
45. Pedersen H. Absence of dynein arms in endometrial cilia: cause of infertility? Acta Obstet Gynecol Scand 1983; 62:625–627.